ISSN 1063-7834, Physics of the Solid State, 2021, Vol. 63, No. 4, pp. 654–659. © Pleiades Publishing, Ltd., 2021.
ISSN 1063-7834, Physics of the Solid State, 2021. © Pleiades Publishing, Ltd., 2021.
Russian Text © The Author(s), 2021, published in Fizika Tverdogo Tela, 2021, Vol. 63, No. 4, pp. 545–549.

Synthesis and Structural, Magnetic, and Thermal Properties of the Titanium-Doped $Pb_3Mn_7O_{15}$ Compound

S. N. Sofronova[a], *, E. V. Eremin[a], M. S. Molokeev[a], N. V. Mikhashenok[a], and A. V. Kartashev[a]

[a] *Kirensky Institute of Physics, Krasnoyarsk Scientific Center, Siberian Branch, Russian Academy of Sciences, Krasnoyarsk, 660036 Russia*

**e-mail: ssn@iph.krasn.ru*

Received December 4, 2020; revised December 4, 2020; accepted December 7, 2020

Abstract—The $Pb_3Mn_7O_{15}$ crystals doped with titanium ions have been synthesized. The study of the structural properties has shown that titanium ions occupy positions in the interplane columns, which weakens the exchange coupling between the planes. Two anomalies in the temperature dependences of magnetization and heat capacity at 62 and 35 K have been found. It has been supposed that, at 62 K, the long-range magnetic order arises and, at 35 K, a spin-reorientation transition, as in the $Pb_3Mn_7O_{15}$ compound, occurs.

Keywords: manganites, magnetic phase transition, indirect exchange coupling

DOI: 10.1134/S1063783421040223

1. INTRODUCTION

The compounds containing one element in different valence states attract close attention of researchers due to their intriguing physical properties and application potential. Such compounds are often met among manganites, since manganese can be in different (2+, 3+, or 4+) valence states.

The compounds with a perovskite-like structure are best studied; however, there are other families of compounds containing manganese in different valence states. Among them is $Pb_3Mn_7O_{15}$ [1–4]. Manganese is included in this compound in two valence states, 3+ and 4+, in a ratio of 4 : 3. The structure of this compound has been discussed for a certain period of time and, according to some data, was found to be orthorhombic (*Pnma*) [2] and, according to other data, hexagonal (*P*63/*mcm*) [3]. The main structural feature of this compound is the presence of planes interconnected by columns (Fig. 1). Kimber et al. [4] showed the occurrence of a structural phase transition between the hexagonal and rhombic structures, which is caused by the charge and orbital orderings. Three anomalies were found in the magnetization curves of the $Pb_3Mn_7O_{15}$ compound. The first anomaly at 160 K is related to the cluster-type isotropic ordering; the second, at 70 K, to the onset of a long-range magnetic order; and, the third, at 20 K, to the spin-reorientation transition [3]. Recently, the magnetic structure of this compound was determined, which appeared rather complex [5]. The magnetic moments of manganese ions in different symmetry positions are noncollinear.

Partial substitution of various magnetic and nonmagnetic ions for manganese ones significantly changes the transport, magnetic, and structural properties. In particular, the Fe^{3+} and Rh^{3+} inclusions stabilize the hexagonal structure [6, 7]. The Ga^{3+} and Ge^{4+} inclusions stabilize the orthorhombic structure [1]. The inclusion of nickel ions lowers the symmetry to *P*3*c*1 [8].

The magnetic properties significantly change upon doping with iron by more than 10%: the system passes to the spin-glass state and the long-range magnetic order vanishes [6]. Upon nickel and gallium doping, the transition at 160 K disappears and the long-range magnetic order arises at 65 and 60 K, respectively [1, 8]. Germanium doping (5 at %) almost does not affect the magnetic properties [1].

In this work, we report on the investigations of the structural, magnetic, and thermal properties of the $Pb_3Mn_7O_{15}$ compound doped with titanium ions.

2. EXPERIMENTAL

The investigated $Pb_3Mn_{7-x}Ti_xO_{15}$ ($x = 0.05$) single crystals were grown by spontaneous crystallization from flux. The presence of PbO in the composition allowed us to use this oxide as a solvent. This made it possible to avoid contamination of the crystals with foreign impurities and to obtain high-quality crystals. The initial components were high-quality PbO, Mn_2O_3, and TiO_2 oxides taken in a desired ratio. The component mixture was placed in a platinum crucible, heated to 1000°C, and kept at this temperature for 4 h

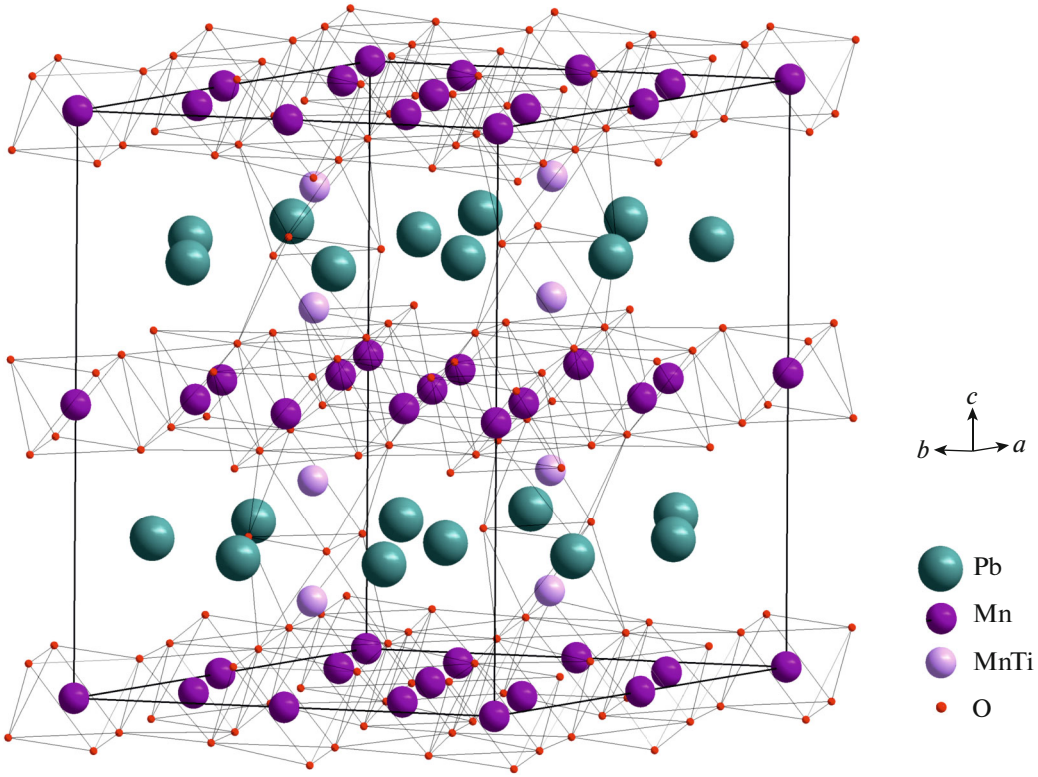

Fig. 1. Crystal structure of the $Pb_3(Mn,Ti)_7O_{15}$ compound.

until the flux was completely homogenized. After that, the crucible with the charge was cooled down to 900°C at a rate of dT/dt = 2–5°C/h. Then, the furnace was switched off and cooled down to room temperature. Single crystals were mechanically withdrawn from the crucible. The synthesized single crystals were plate-like and had a smooth black surface. The plate sizes were up to 2–4 mm.

3. STRUCTURAL PROPERTIES

The X-ray powder diffraction study was carried out on a Bruker D8 ADVANCE diffractometer. The experimental and lattice parameters are given in Table 1. The coordinates of atoms and their distribution over positions are given in Table 2. Table 3 gives the distances between the metal and oxygen ions.

We expected that titanium doping, similar to germanium doping, would stabilize the orthorhombic structure and titanium ions would replace manganese ones in the planes [1]. However, in contrast to the case of $Pb_3Mn_{7-x}Ge_xO_{15}$, substitution of titanium for manganese led to the stabilization of the hexagonal structure. Titanium ions occupied positions in columns between the planes. In $Pb_3Mn_7O_{15}$, these positions are predominantly occupied by trivalent manganese. Titanium ions can be included in the crystal in both the tetra- and trivalent state. Tetravalent titanium ions are nonmagnetic, in contrast to trivalent titanium. The valence state of an ion in a crystal is difficult to determine; meanwhile, the valence state of titanium should noticeably affect the magnetic properties of the compound under study.

Table 1. Parameters of the experiment and lattice parameters of the $Pb_3(Mn,Ti)_7O_{15}$ compound

M_r = 1241 (4)	Z = 4
Hexagonal, $P6_3/mcm$	D_x = 6.978 Mg m^{-3}
a = 10.0140 (2) Å	Cu$K\alpha_{12}$ radiation, α = 1.5406, 1.5443 Å
c = 13.6034 (4) Å	T = 300 K
V = 1181.38 (6) Å^3	
D8 ADVANCE Bruker diffractometer	Scan method: step
Data collection mode: reflection	$2\theta_{min}$ = 8.00°, $2\theta_{max}$ = 140.00°, $2\theta_{step}$ = 0.02°
R_p = 2.985	8250.4545 data points
R_{wp} = 4.129	Profile function: PearsonVII
R_{exp} = 1.602	Preferred orientation correction: Anisotropic model of PO. Spherical harmonics 2 order. [9]
R_{Bragg} = 1.97	

Table 2. Atomic coordinates and occupancies of the positions in the $Pb_3(Mn,Ti)_7O_{15}$ compound

Atom	x	y	z	B^*_{iso}/B_{eq}	Occ. (<1)
Pb1	0.6114 (2)	0.6114 (2)	0.75	2.59 (7)	1
Pb2	0.2644 (2)	0.2644 (2)	0.75	3.41 (9)	1
Mn1	0.8322 (3)	0.1678 (3)	0.5	1.8 (2)	1.00 (13)
Ti1	0.8322 (3)	0.1678 (3)	0.5	1.8 (2)	0.00 (13)
Mn2	0.333333	0.666667	0.1472 (5)	0.71 (18)	**0.64 (11)**
Ti2	0.333333	0.666667	0.1472 (5)	0.71 (18)	**0.36 (11)**
Mn3	0.5	0.5	0.5	1.6 (3)	1.00 (21)
Ti3	0.5	0.5	0.5	1.6 (3)	0.00 (21)
Mn4	0	0	0	2.5 (5)	1.00 (28)
Ti4	0	0	0	2.5 (5)	0.00 (28)
O1	0.4847 (17)	0.3319 (15)	0.0808 (12)	4.4 (3)	1
O2	0.519 (3)	0.170 (2)	0.25	4.4 (3)	1
O3	0.156 (2)	0.156 (2)	0.0719 (15)	4.4 (3)	1
O4	0.673 (2)	0.673 (2)	0.0658 (16)	4.4 (3)	1

The position occupied by an ion upon substitution is, probably, determined by the ionic radius of a dopant, rather than its valence state. The Ge^{4+} ionic radius is merely 0.044 nm, while the Ga^{3+}, Ti^{4+}, Fe^{3+}, and Ni^{2+} ionic radii are 0.062, 0.064, 0.067, and 0.078 nm, respectively. The Mn^{3+} and Mn^{4+} ionic radii are 0.052 and 0.07 nm, respectively. Since the in-plane crystallographic positions are mainly occupied by tetravalent manganese, the ionic radius of which is smaller than the that of trivalent manganese, the germanium ion with the smallest radius occupies the in-plane positions, while the larger ions, regardless of their valence, occupy positions between the planes, which are predominantly occupied by trivalent manganese.

Table 3. Me–O bond lengths (Å)

Pb1–O1^{i}	2.663 (15)	Mn2–O1^{vi}	2.027 (13)
Pb1–O2^{ii}	2.30 (2)	Mn2–O2^{vii}	2.099 (15)
Pb2–O2^{ii}	2.25 (2)	Ti2–O1^{vi}	2.027 (13)
Pb2–O4^{i}	2.58 (2)	Ti2–O2^{vii}	2.099 (15)
Mn1–O1^{iii}	1.920 (14)	Mn3–O1^{viii}	1.951 (14)
Mn1–O3^{iv}	2.000 (20)	Mn3–O4^{viii}	1.950 (18)
Mn1–O4^{v}	1.867 (18)	Ti3–O1^{viii}	1.951 (14)
Ti1–O1^{iii}	1.920 (14)	Ti3–O4^{viii}	1.950 (18)
Ti1–O3^{iv}	2.000 (20)	Mn4–O3	1.840 (19)
Ti1–O4^{v}	1.867 (18)	Ti4–O3	1.840 (19)

Symmetry positions: (i) $-x+1, -y+1;$, $-z+1$; (ii) $x-y, x, -z+1$; (iii) $-x+y+1, y, z+1/2$; (iv) $x+1, -x+y, -z+1/2$; (v) $-x+y+1, -x+1, -z+1/2$; (vi) $x+1, -x+y+1, z$; (vii) $-x+1, -x+y+1, -z+1/2$; (viii) $x+1, -y+1, z+1/2$.

4. RESULTS AND DISCUSSION

The magnetization was measured on a Quantum Design Physical Properly Measurement System (PPMS). Figure 2 shows temperature dependences of magnetization in a field of $H = 500$ Oe applied along the c axis (blue asterisks) and in the ab plane (closed and open circles). The in-plane measurements were performed in the zero-field cooling (ZFC) and field-cooling (FC) modes. The magnetization curves have two features observed at 62 and 35 K. For the $Pb_3Mn_7O_{15}$ compound, there is a broad smoothed peak around 140 K, while for $Pb_3(Mn,Ti)_7O_{15}$, it is not observed. At a temperature of 62 K, the magnetic ordering is established and, at 35 K, a spin-reorientation transition probably occurs. The behavior of the magnetization of the $Pb_3(Mn,Ti)_7O_{15}$ compound is very similar to that of $Pb_3(Mn,Ga)_7O_{15}$. In both compounds, the temperature of the magnetic ordering is 62 K. In both compounds, the ion replaces manganese ions in the interplane columns. Trivalent gallium ions are nonmagnetic; this weakens the exchange coupling between the layers. Probably, in the investigated compound, the ions in the tetravalent state are also nonmagnetic. However, since the dopant ions in $Pb_3(Mn,Ga)_7O_{15}$ and $Pb_3(Mn,Ti)_7O_{15}$ have different valences, Mn^{3+} and Mn^{4+} should be redistributed in the planes, differently for the two compositions.

In addition, we performed the heat capacity measurements using an adiabatic setup, which is a simplified adiabatic calorimeter without an external thermo-

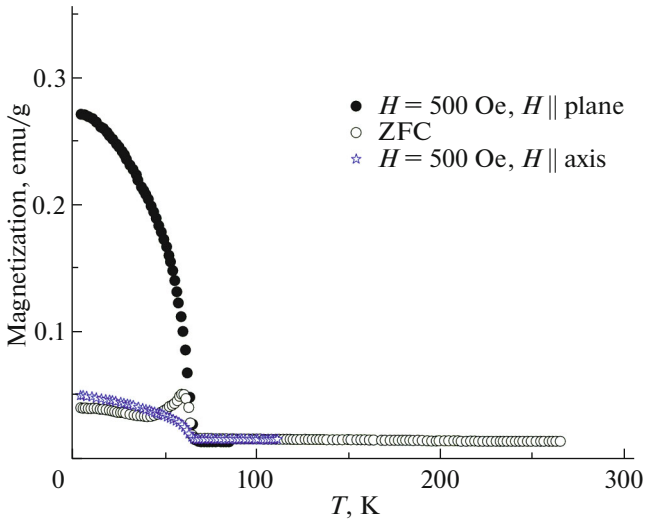

Fig. 2. Temperature dependences of magnetization in a field of $H = 500$ Oe applied along the c axis (blue asterisks) and in the ab plane (closed and open circles).

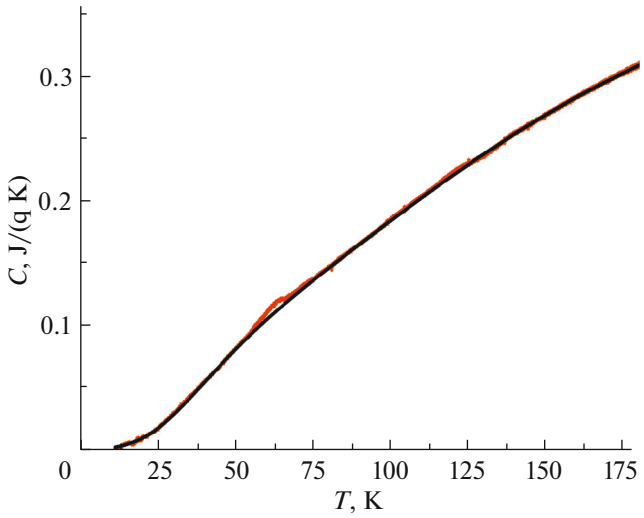

Fig. 3. Temperature dependences of heat capacity. The red line corresponds to the sample and the black line, to the lattice contribution.

static screen (for more detail, see [10]). The measurements were performed in the range from 15 to 300 K. At temperatures of 15–100 K, the cryostat was immersed in a bath with liquid helium and, above 100 K, in a bath with liquid nitrogen.

The sample was a tablet placed in an aluminum cell with a mass of 125.2 mg; the thermal contact was ensured with Apiezon N vacuum grease. The heat capacity of the cell and the vacuum grease was determined in a separate experiment and taken into account in calculating the heat capacity of the investigated sample.

Figure 3 shows temperature dependences of the heat capacities of the sample and the lattice. The heat capacity of the lattice was determined using a linear combination of the Debye and Einstein functions by the least-squares method from the heat capacity data, excluding the temperature range of 50–90 K, which corresponds to the anomalous portion. The Debye and Einstein temperatures were $a_1 = 239$ K and $a_3 = 574$ K with weight coefficients of $a_0 = 0.61$ and $a_2 = 0.27$, respectively.

$$f(x,a) = a_0\left(\frac{x}{a_1}\right)^3\int_0^{\frac{a_1}{x}} t^4\frac{\exp(t)}{(\exp(t)-1)^2}dt + a_2\left(\frac{a_3}{x}\right)^2\frac{\exp\left(\frac{a_3}{x}\right)}{\left(\exp\left(\frac{a_3}{x}\right)^{-1}\right)^2}.$$

The difference between the total and lattice heat capacities was used to obtain the heat capacity containing two diffuse anomalies with maxima at temperatures of 62 and 35 K (Fig. 4). The temperature dependence of the entropy was calculated using the anomalous heat capacity. The entropies of the phase transformations were found to be 1.5 mJ/(q K) and 0.5 mJ/(q K) at 62 and 35 K, respectively.

Based on the analysis of the exchange magnetic structure of $Pb_3Mn_7O_{15}$ [5], we estimated the exchange couplings in $Pb_3(Mn,Ti)_7O_{15}$. We assumed that titanium ions entered the compound in the tetravalent state and the trivalent and tetravalent manganese ions were distributed over the positions (Table 4) taking into account the experimental mag-

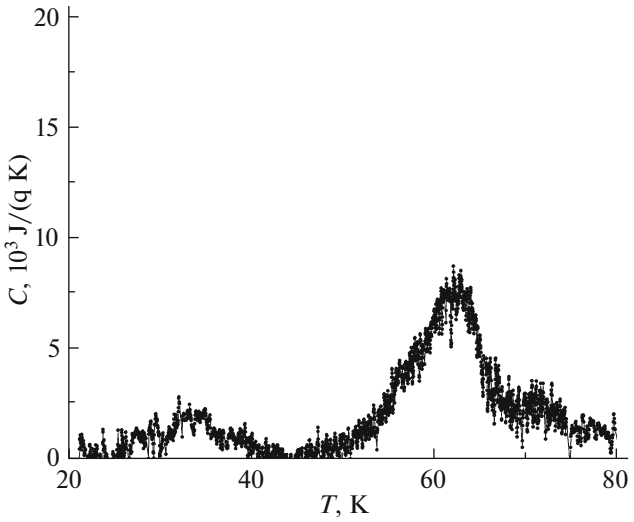

Fig. 4. Anomalous portion of the heat capacity.

Table 4. Occupancies of the positions by Mn^{3+}, Mn^{4+}, and Ti^{4+} ions

Symmetry position	Mn^{3+}	Mn^{4+}	Ti^{4+}
6*f*	1.0	–	–
8*h*	0.64	–	0.36
12*i*	0.445	0.555	–
2*b*	–	1.0	–

Table 5. Comparison of the exchange couplings in $Pb_3(Mn, Ti)_7O_{15}$ and $Pb_3Mn_7O_{15}$

Positions	12*i*–6*f*	12*i*–12*i*	12*i*–2*b*	12*i*–8*h*	6*f*–8*h*	8*h*–8*h*
$Pb_3(Mn,Ti)_7O_{15}$ J(K)	–5.4	–4.9	–5.5	–1.1	–1.3	–6.3
$Pb_3Mn_7O_{15}$ J(K) [1]	–8.5	–6.9	–3.9	–1.2	–3.4	–15.4

netic structure of $Pb_3Mn_7O_{15}$ and the Me–O bond lengths in the $Pb_3(Mn,Ti)_7O_{15}$ compound (Table 3).

To calculate the exchange couplings with allowance for the occupancies of different positions by the tri- and tetravalent manganese ions, we used the values of exchange couplings obtained in [1]. The values of the exchange couplings are given in Table 5. The presence of nonmagnetic ions in the interplane columns (position 8*h*) significantly weakens the interplane exchange coupling. However, all the in-plane exchange couplings remain antiferromagnetic and strongly frustrated, since the exchange paths form triangular groups.

The regions with the short-range order, which occur around 140 K, are probably connected to the interplane positions; when the latter are occupied by a nonmagnetic ion or another magnetic ion, the formation of such regions becomes impossible. For example, in $Pb_3(Mn,Ge)_7O_{15}$, a feature in the range of 140–160 K remains, since germanium ions occupy the in-plane positions, whereas in $Pb_3(Mn,Ga)_7O_{15}$, $Pb_3(Mn,Ti)_7O_{15}$, and $Pb_3Mn_{5.5}Ni_{1.5}O_{15}$ it vanishes.

The arrangement of ions in the *ab* plane is similar to the Kagome structure and, since all the in-plane exchange couplings are antiferromagnetic and have similar values, this leads to the strong frustrations. As a result of the frustrations, the magnetic moments in most positions in $Pb_3Mn_7O_{15}$ are noncollinear and the angles between them are close to 60° and 120° [5]. Since the temperature dependences of the magnetization of $Pb_3(Mn,Ti)_7O_{15}$ measured in a field applied in the *ab* plane and along the *c* axis at temperatures below 62 K are similar to the temperature dependences of the magnetization of $Pb_3Mn_7O_{15}$, we assume that the long-range magnetic order in $Pb_3(Mn,Ti)_7O_{15}$ will be similar to the magnetic order in $Pb_3Mn_7O_{15}$.

5. CONCLUSIONS

Thus, we reported on the synthesis of the $Pb_3Mn_7O_{15}$ compound doped with titanium ions and study of their structural, magnetic, and thermal properties. It was found that titanium ions occupy positions in the columns between the planes, which weakens the exchange coupling between the latter. Two anomalies, at 62 and 35 K, was found in the temperature dependences of magnetization and heat capacity. At 62 K, the long-range magnetic order presumably arises and, at 35 K, a spin-reorientation transition, as in $Pb_3Mn_7O_{15}$, occurs.

ACKNOWLEDGMENTS

This study was carried out on the equipment of the Krasnoyarsk Regional Center for Collective Use, Krasnoyarsk Scientific Center, Siberian Branch of the Russian Academy of Sciences.

FUNDING

This study was supported by the Russian Foundation for Basic Research, the Government of the Krasnoyarsk krai, and the Krasnoyarsk Territorial Foundation for Support of Scientific and R&D Activities, project no. 18-42-240007.

CONFLICT OF INTEREST

The authors declare that they have no conflicts of interest.

REFERENCES

1. E. V. Eremin, N. V. Volkov, K. A. Sablina, O. A. Bayukov, M. S. Molokeev, and V. Yu. Komarov, J. Exp. Theor. Phys. **124**, 792 (2017).
2. J. C. E. Rash, D. V. Sheptyakov, J. Schefer, L. Keller, M. Boehm, F. Gozzo, N. V. Volkov, K. A. Sablina, G. A. Petrakovskii, H. Grimmer, K. Conder, and J. F. Löffler, J. Solid State Chem. **182**, 1188 (2009).

3. N. V. Volkov, L. A. Solovyov, E. V. Eremin, K. A. Sablina, S. V. Misjul, M. S. Molokeev, A. I. Zaitsev, M. V. Gorev, A. F. Bovina, and N. V. Mihashenok, Phys. B (Amsterdam, Neth.) **407**, 689 (2012).

4. S. A. J. Kimber, J. Phys.: Condens. Matter. **24**, 186002 (2012).

5. S. A. Ivanov, A. A. Bush, M. Hudl, A. I. Stash, G. Andre', R. Tellgren, V. M. Cherepanov, A. V. Stepanov, K. E. Kamentsev, Y. Tokunaga, Y. Taguchi, Y. Tokura, P. Nordblad, and R. Mathieu, J. Mater. Sci.: Mater. Electron. **2**, 12562 (2016).

6. N. V. Volkov, E. V. Eremin, O. A. Bayukov, K. A. Sablina, L. A. Solov'ev, D. A. Velikanov, N. V. Mikhashenok, E. I. Osetrov, J. Schefer, L. Keller, and M. Boehmd, J. Magn. Magn. Mater. **342**, 100 (2013).

7. A. J. Gatimu, H. Mizoguchi, A. Sleight, and M. A. Subramanian, J. Solid State Chem. **183**, 866 (2010).

8. T. I. Milenov, P. M. Rafailov, V. Tomov, R. P. Nikolova, V. Skumryev, J. M. Igartua, G. Madariaga, G. A. López, E. Iturbe-Zabalo, and M. M. Gospodinov, J. Phys.: Condens. Matter **23**, 156001 (2011).

9. M. Jarvinen, J. Appl. Crystallogr. **26**, 525 (1993).

10. A. V. Kartashev, I. N. Flerov, N. V. Volkov, and K. A. Sablina, Phys. Solid State **50**, 2115 (2008).

Translated by E. Bondareva